Received: July 5, 2022. Revised: August 31, 2022.

International Journal of
Intelligent Engineering & Systems

http://www.inass.org/

PV Farm Ancillary Function for Voltage Sag Mitigation Caused by Inrush Current of an Induction Motor

Indra Budi Hermawan[1,2] **Mochamad Ashari[1]*** **Dedet Candra Riawan[1]**

[1]*Department of Electrical Engineering, Institut Teknologi Sepuluh Nopember, Surabaya 60111, Indonesia*
[2]*Department of Electrical Technology, Faculty of Vocations, Universitas 17 Agustus 1945 Surabaya 60118, Indonesia*
* Corresponding author's Email: ashari@ee.its.ac.id

Abstract: This paper presents a control technique for sag voltage mitigation by utilizing PV farm. PV farm has become a preferred green energy source to be installed in industries for the last decades, especially to meet the Sustainable Development Goal programs. The proposed technique is to incorporate PV farm to compensate sag voltages particularly caused by the inrush current of an induction motor starting. The ancillary function of the PV farm is carried out by adding a supercapacitor (SC). PV and SC are used to provide high power in short period when an inrush current occurs. Power from PV and SC is controlled using a current-controlled voltage source inverter which is synchronized with current drawn by induction motor. As the result, PV farm is capable to inject a portion of current into the grid to reduce level of voltage sag. The portion of energy absorbed causing the sag is then calculated and tabulated. A control with a proportional and integral controller is used for sag compensations. A simplified medium-voltage industrial network with a complex load and the induction motor is simulated to validate the proposed method. Simulation result shows that the proposed technique decreases the magnitude of the voltage sag, from 6.71 % to less than 5 %. Sag duration of the voltage sag was also reduced from 5.3 seconds to 4.9 seconds. Thus, the voltage quality can be maintained within the standard requirement. Simulations are also carried out in industrial production processes, where two induction motors are started in close time intervals. The second motor is started a few seconds after the first motor has reached its nominal speed. The result suggested that the voltage on the system bus can be maintained at a level above 6.27 at a nominal system voltage of 6.6 kV. Performance of the proposed technique is capable in maintaining power quality in the studied plant.

Keywords: Power quality, Voltage sag, Voltage source inverter, PV farm, Super capacitor.

1. Introduction

Voltage sag has been a critical concern in the industrial environment. Many damages and stability problems that caused the interruption of the production process have been reported due to the occurrence of voltage sags. One of the contributors to the voltage sag is the starting of a large induction motor at a medium voltage (MV) level. Voltage at buses of the distribution system is greatly influenced by the impedance of the power transformer and of inrush current of the MV motor connected to the bus. If the power supply is not strong enough to bear the inrush current of the motors, the voltage sag will be more severe [1, 2]. While induction motors offer many advantages over the other types of prime mover, it also has considerations that require an immediate solution. This requirement then becomes the code or regulation to assure the power quality in the area [3, 4].

Many studies have been carried out to identify a safe and efficient method for starting large MV induction motors without compromising the network voltage level. Previous research to overcome this problem started with conventional methods such as autotransformers and conventional methods [5, 6]. Along with technological developments, the next

research is the use of flexible AC transmission system (FACTS) devices. FACTS devices used to solve this problem include static compensator (Statcom), dynamic voltage restorer (DVR), and unified power quality conditioner (UPQC) [7].

Other researches that use FATCS devices to solve motor starting problems are transient-free capacitor switching (TFCS) [8] and thyristor controlled series capacitor (TCSC) [9]. These methods utilize the advantages of capacitors combined with various controllers.

When an inrush current occurs, reactive power is absorbed in large quantities and in a short time. The most researched method to be able to compensate for this reactive power requirement is to use a static compensator (STATCOM). In a Statcom, reactive power exchange between the device and the AC system. When an induction motor is started and the voltage sag occurs, the Statcom will inject the reactive power into the AC system. This reactive power injection will reduce the magnitude of the voltage sag, as some portion of the reactive power is supplied by Statcom. Various studies on the use of Statcom have been carried out [10-14].

Dynamic voltage restorer (DVR) is also known as an effective method for mitigating power quality disturbances in the form of sag and swell voltages [15-17]. In the event of voltage sag, DVR will inject the appropriate voltage required into the supply bus to compensate for the sag. It acts as a buffer to the load and mitigates unacceptable disturbances. This DVR is installed on the switchgear in series and between the power supply and the load.

Starting a large MV induction motor will draw a large amount of active and reactive power from the network; therefore, the injection of active and reactive power into the network is widely researched. Research in this field has resulted in various control methods and inverter topologies [18-21]. With the advancement of power electronic devices and control techniques, research is also being done on the utilization of energy storage media as an external power source. Among the achievements of the current development of energy storage media technology, Super capacitors are the choice of many researchers [22-25].

Integrations of energy storage, inverter, and control become important to overcome power quality problems. The research that has been done for this integration shows significant achievements [26-31].

This paper proposes a method to increase voltage stability of electrical power systems in an industrial application by utilizing PV farm as an external power source. A typical MV distribution system consisting of a power transformer, static loads, and large induction motors of 2500 hp and 4500 hp is used as a study case. PV farm is incorporated to supply 30% of the internal load demand of the plant.

The plant is supplied by 20/6.6-kV power transformer. The 20-kV bus will suffer from voltage sag when the DOL starting of the induction motor is taking place. Therefore, the compensation technique is applied to reduce voltage sag by utilizing the active and reactive power support function of the PV farm power converters.

Since PV is modeled as a constant current source, a supercapacitor (SC) is inserted in the power converter system to handle large power in very short duration during motor starting. Under normal conditions, the PV farm is operated in MPPT mode. Prior to motor starting process, the PV voltage is controlled at a specific value to charge the SC. With a particular voltage regulation, this supercapacitor functioned as energy storage. The energy stored in this capacitor is then fed to the current controlled voltage source inverter (CC-VSI), which detects the starting of the induction motor based on the motor's rotational speed. Average current mode control is used to adjust the output voltage of the voltage source inverter. The controller senses the amplitude and phase of motor current as a reference for the controller of CC-VSI. This reference signal is then compared with the converter output current and fed to the PI controller. The result is a modulated signal for the VSI.

The rest of the paper is organized as follows: section 2 focuses on modeling the system, including the PV Farm system, supercapacitor, and industrial plant. The test system and method for evaluating small signal stability are described in section 3. The simulation results are presented and discussed in section 4. Eventually, the conclusions of this paper are addressed in section 5.

2. System modelling

A single-line diagram represents the entire system study, as shown in Fig. 1. This plant is connected to a 6.6-kV bus which is supplied by a power transformer rated at 8.5 MVA, 20/6.6-kV with 7.5 % impedance. Large induction motors are connected to a 6.6-kV MV bus. Meanwhile,

supporting systems such as cooling tower systems, transfer pumps, filling stations, and office equipment are connected to the LV distribution board which is supplied by a utility 6.6/0.4-kV transformer.

This load becomes the initial load of the plant before it is fully operational. The operation of the system is explained as follows. After all the LV loads

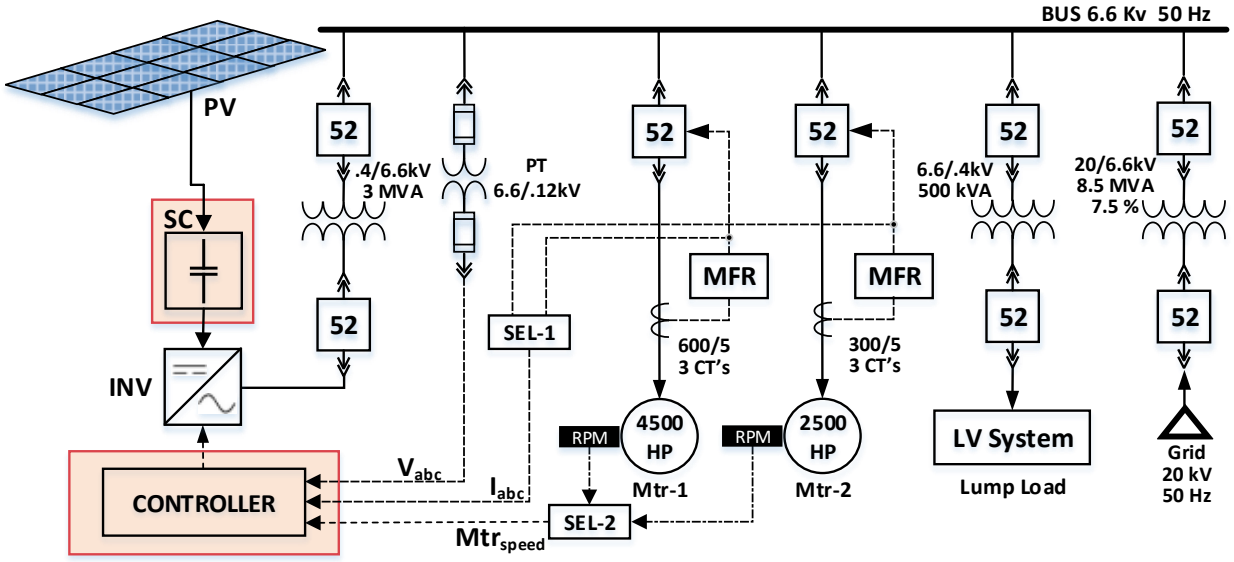

Figure. 1 Single line diagram of the system study

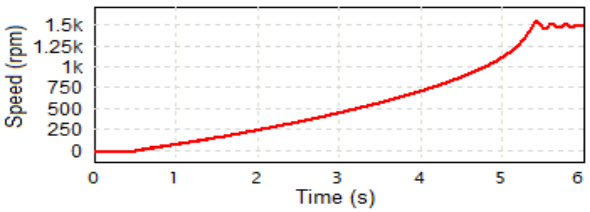

(a)

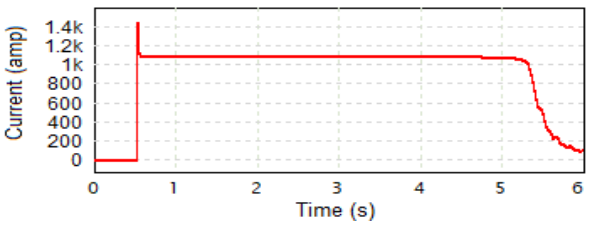

(b)

Figure. 2 Starting of 4500 HP: (a) Motor speed and (b) Motor current

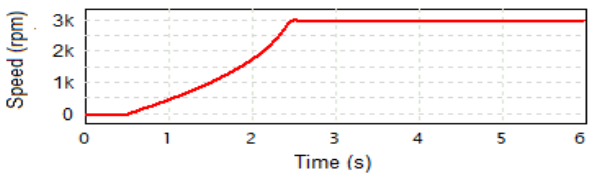

(a)

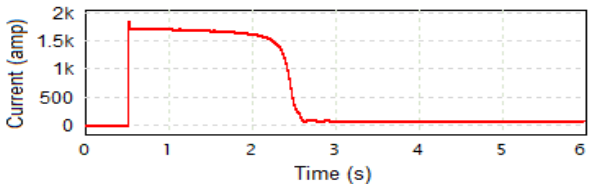

(b)

Figure. 3 Starting of 2500 HP: (a) Motor speed and (b) Motor current

are operated, the medium voltage motor's support system is executed. This system includes the motor lubrication, cooling system, and instrumentation equipment used in the medium voltage motor. The first motor that is run is Mtr-1 as the main motor for the production process, then it is followed by Mtr-2 as a further driving motor. Operational records show that MV bus always experiences a voltage sag when the MV motor is started.

PV Farm and SC are modeled as a constant current source and simple large capacitor respectively. A capacitor is inserted in dc bus of VSI of 1000 WP PV farm system. In normal operation, PV farm is intended to provide about 30% of the electrical power requirement. PV and SC feed their energy to the grid using VSI via a step-up transformer of 3-MVA, 0.4/6.6-kV. Controller of VSI receives motor current. signal forming a reference current. This reference is then used by VSI to inject precise compensation current into the grid.

The parameter of the induction motor used in this study is obtained from manufacturer testing data in the datasheet. The datasheet includes both steady-state and transient impedances, time constant, and inertia constant.

2.1 Simulated induction motor starting current

This study uses practical data of MV induction motor obtained from the actual plant. The plant has two MV induction motors. The first motor is Mtr-1, a 4500 HP 6,6 kV 1491 rpm, and the second motor is Mtr-2, a 2500 HP 6.6 kV 2980 rpm. These two induction machines are the key to the plant operation, running consecutively between Mtr-1

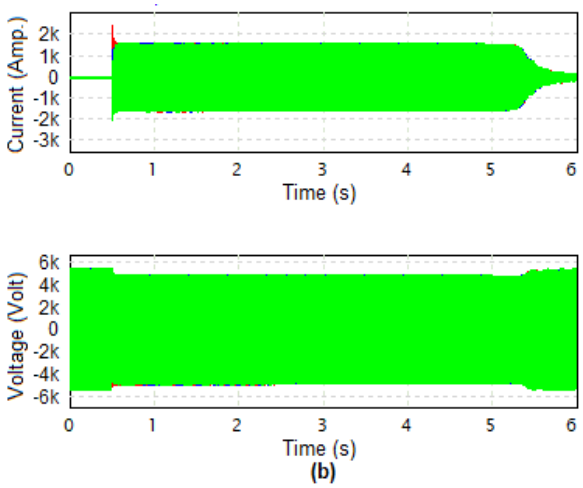

Figure. 4: (a) Grid current and (b) Voltage during 4500 HP motor starting.

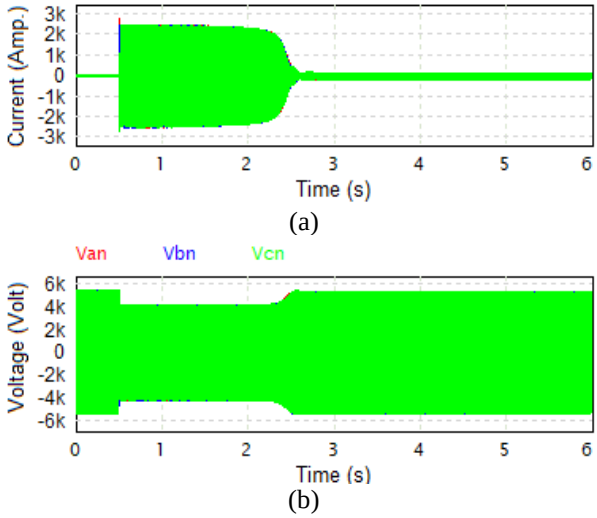

Figure. 5: (a) Grid current and (b) Voltage during 2500 HP motor starting

and Mtr-2. The simulated starting current of motors and its impact on bus voltage is shown in Fig. 2 and Fig. 3. Peak values of starting current 1,077 A-rms and 1,669 A-rms for Mtr-1 and Mtr-2 respectively. These current cause 11.98 % and 25.16 % voltage drop at 6.6-kV bus as shown in Fig. 4 and Fig. 5. It can be noted that starting of MV motors causes severe voltage sag. Since voltage sag are more than 5%, it becomes a concern to power quality in the studied system.

2.2 Super capacitor sizing

Capacitance of SC is calculated by considering dc bus voltage range and modulation index of the voltage source inverter (VSI). Eqs. (1) to (3) are used to determine appropriate size of the SC. This SC final voltage is the voltage at the SC terminal

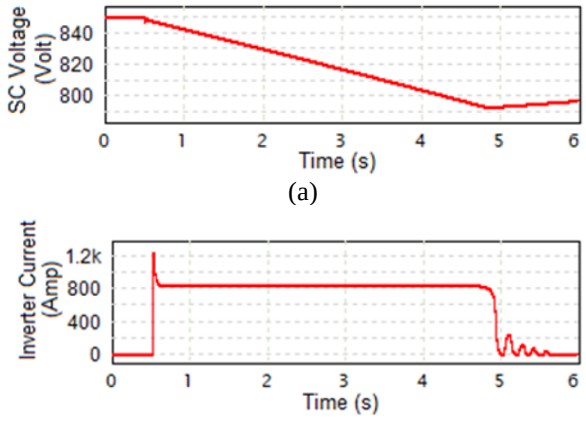

Figure. 6: (a) Supercapacitor voltage during motor starting and (b) Inverter during motor starting

just after the SC supplies electrical energy to the inverter. The modulation index is defined as the ratio of the fundamental component amplitude of the line-to-neutral inverter output voltage to one-half of the available dc bus voltage. For a VSI, the maximum allowable modulation index (m_a) value can be calculated using the following equation [32]:

$$\hat{v}_{ab1} = m_a\sqrt{3}\,\frac{V_i}{2} \quad (0 < m_a \leq \frac{2}{\sqrt{3}}) \tag{1}$$

Where $\hat{v}_{ab1}$ is the peak voltage of the AC input, m_a represents the inverter modulation index and V_i denotes the dc voltage of the supercapacitor. From Eq. (1), the modulation index can be calculated as follows:

$$m_a = 2\,\frac{\hat{v}_{ab1}}{\sqrt{3}\,V_i} \tag{2}$$

so the dc voltage equation (V_i) becomes:

$$V_i = 2\,\frac{\hat{v}_{ab1}}{\sqrt{3}\,m_a} \tag{3}$$

In this simulation, the inverter's rated input and output voltages are 1000 Volts (dc) and 440 Volts (dc) respectively. A Step-up transformer is used to increase the inverter output voltage to 6.6-kV.

From the calculation of Eqs. (2) and (3), we can have the modulation index (m_a) = 0.72, and the final dc voltage (V_i) at the supercapacitor = 756 Volt. Hence we have the delta voltage at the supercapacitor is 244 and the electric charge at the supercapacitor = 60,917 Coulomb. From the calculation, we also can see that the energy required for the compensation is 7,421,660 Joule, or equal to 2.062 kWh.

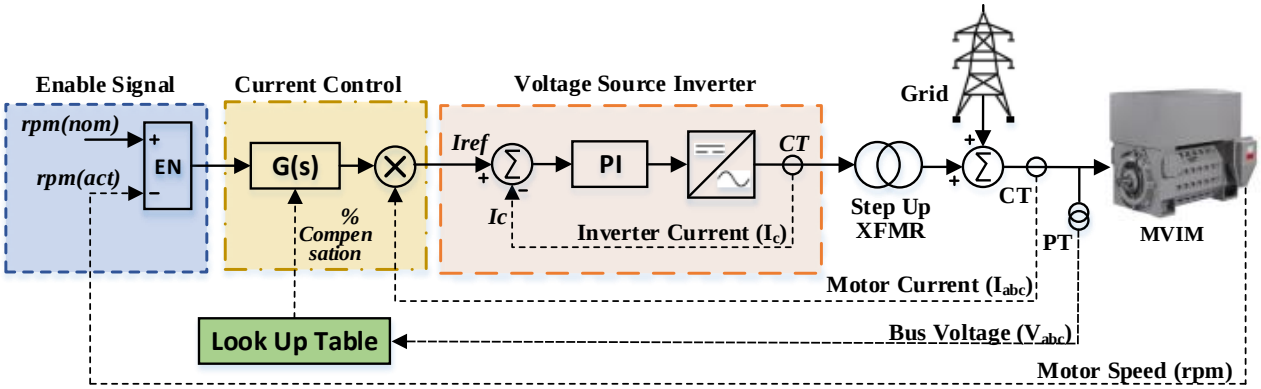

Figure. 7 Controller block diagram

Simulation shows that the minimum allowable supercapacitor value is above 750 Vdc. If this final voltage falls below 750 Volt, the inverter output voltage will not be strong enough to mitigate excess electric current when an inrush current occurs. Fig. 6 shows the graph of the SC voltage drop used in this study. By using a 250 Farad 1000 Volt Supercapacitor, the final supercapacitor voltage when used to compensate for the inrush current Mtr-2 is 792 Vdc. This final voltage is used to compensate the inrush current of a 4500 hp MVIM at 70 % compensation.

2.3 Power injection to the bus

Integration of renewable-based power generation creates novel challenges in the planning and operation of the plant power system. From a load-flow point of view, this ancillary function of the PV will change the operation mode of the electrical system in the industrial plant. Under normal conditions, the energy generated by PV will be fully directed to the plant to reduce some of the plant load. However, when starting a large induction motor, the energy from the PV will be used to charge the supercapacitor. The main procedure for implementing the compensation method to mitigate voltage sag under variations of induction motor size in an industrial plant is given as follows:

- Determine the sag voltage and supercapacitor capacity to supply the shortfall in electrical energy that occurs at the time of the inrush current.
- Determine the inverter modulation index so that there is no over or under modulation
- Setup controller to determine the percentage of inrush current compensation
- Start the motor, confirm the sag voltage is acceptable, and record the final voltage of the supercapacitor
- Recalculate the modulation index, voltage, and capacity of the supercapacitor.

When starting the motor, the process that occurs in the controller is receiving the enable signal from the speed sensor, receiving motor current from the current sensor (CT), processing input data for compensation percentage, and issuing modulation data to the inverter.

3. Proposed voltage sag compensator

Based on the sag voltage characteristics caused by the motors, a sag controller is designed. The controller block diagram for this paper is shown in Fig. 7. The first block, namely the Enable Signal, detects when the motor starts. It changes the PV farm to compensate for any inrush current instead of working as a power plant.

The inrush current on the grid occurs when the motor starts moving from 0 rpm until it reaches the nominal speed of the motor. This condition produces three measurement parameters that can be used as input controllers. The three parameters are the motor speed, electrical current absorbed by the motor, and the voltage at Bus 6.6 kV. In this study, the induction motor, which is the object of research, is an induction motor with nominal stator speeds are 1500 rpm and 3000 rpm. The percentage of current injected into the system is determined by the motor's actual speed (rpm) and the amount of current absorbed by the motor. The control variable in grid voltage will be fulfilled according to applicable standards.

The second block, shown in Fig 7, is the current control diagram. This block is for generating the compensated current to be injected into the grid.

Table 1. Lookup up table for voltage sag compensation

Compensation (%)	Voltage Sag (Volt)
10	5965
30	6105
50	6248
70	6390
90	6534

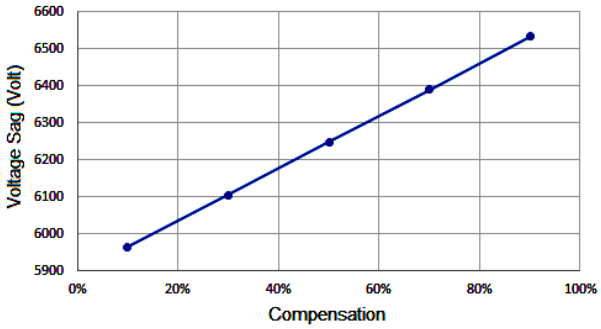

Figure. 8 Lookup table graph, Compensation vs voltage sag for Mtr-1

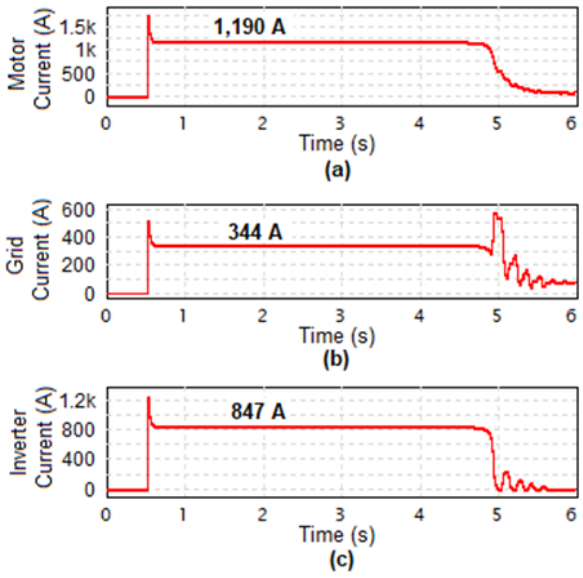

Figure 9. Current's at 70 % compensation: (a) Motor Current (b) Grid current (c) Inverter current

After the motor speed and motor current values are set up in the controller, the next step is to determine the percentage of the current borne by this compensator. It depends on the energy stored in the supercapacitor and the design of the compensation depth. The amount of energy needed for the compensation is known through several experiments. Compensate for the inrush current that occurs. The deep of sags and the compensation needed are then tabulated.

This electrical motor current (Im) signal is obtained from the CT mounted on the motor. The result is a reference current signal (Iref). This iref signal is then compared with the inverter current signal (Ic) as the PI controller input. The PI controller will provide a modulation signal to the inverter. The inverter will produce an AC signal with a current and voltage that can mitigate the inrush current that occurs.

3.1 Lookup table

As mentioned above, the voltage sags and the compensation depth can be obtained from simulations or experiments. Table 1 shows the results for various sags and compensations. Table 1 and Figure 8 suggest that compensation level can be presented either in tabulated data or linear equations (5). Where V_S is the measured bus voltage.

$$C = 711.25\, V_s + 5{,}893.75 \quad (5)$$

VSI in this research is modelled in average model. In the average model, the circuit is simplified, and only the low-frequency behavior is included. Another thing that needs to be considered in the implementation of this compensator is the inverter capacity. The inrush current that occurs will require a very large compensation power in a short time. The compensator should be designed to be able to deliver large amounts of power in a short time.

4. Result and discussion

4.1 System effectiveness

The effectiveness of the control and the system performances under various sag compensations were demonstrated. Fig. 9 depicted the currents at 70 % compensation for the Mtr-1. It shows that the inverter is contributing 847 Amperes which is about 71 % of the Mtr-1 current. Fig. 9 (b) shows that the Grid has borne 344 Ampere to convince the compensation is working as per the design.

Fig. 10 showed the improved voltage sags when the compensations were set at 10 %, 30 %, 50 %, 70 %, and 90 % of the Mtr-1 inrush current. The baseline indicates the sag voltage without any compensations. We can see that without compensation, the voltage drops from 6.6 kV to 5.89 kV which is 10.75 % of the nominal Bus voltage. The voltage sag duration is 5.63 seconds. After the 5th second, the voltage is restored to 6.5 kV. Compensation at 10 % correlates with 5.96 kV. This is slightly improved compared to without any compensation.

When the compensation is set at 90%, the system voltage during the motor starting is shown

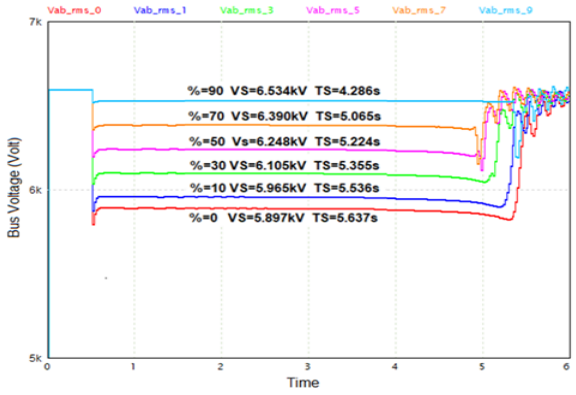

Figure. 10 Magnitude and duration of voltage sag on Mtr-1 with various compensation percentages

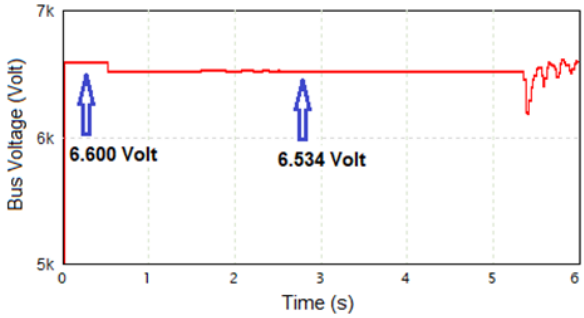

Figure. 11 The system voltage with 90% of compensation results in less than 5 % voltage sag

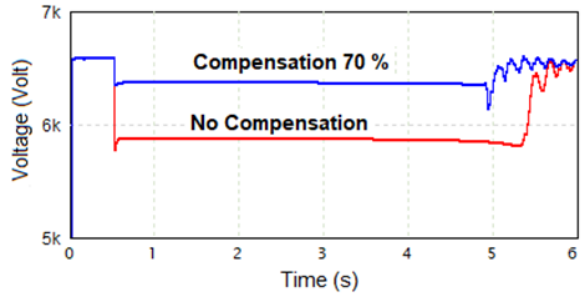

Figure. 12 Voltage sag comparison between 70 % compensation (blue line) and uncompensated starting (red line)

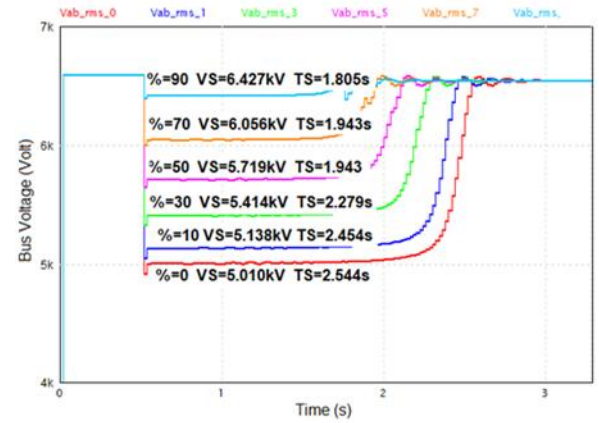

Figure. 13 Magnitude and duration of voltage sag on Mtr-2 with various compensation percentages

in Fig. 11. It can be seen that the voltage is almost restored to the normal voltage. The transient also shows smooth, indicating that the control system is satisfactory.

This study found that a compensation of 70% of the Mtr-1 starting current may bring the quality of the power within the standard. Fig. 12 shows when the compensation is set at 70%, the system voltage during the motor starting is still in the recommended voltage range. 70 % compensation becomes the critical point for Mtr-1 compensation as this compensation is determined whether the system voltage is considered safe or unsafe for the system operation. Below 70 % compensation, the system voltage is considered to experience unexpected voltage sag. Above 70 % compensation, the voltage sag that is sensed is still in the allowable voltage.

Fig. 13 shows the improved voltage sags applied to Mtr-2. This MVIM is a 3000 rpm motor. Hence, we know that this motor has two poles that rotate faster and have a bigger inrush current. The motor modeling depicted in Figs. 4 and 5 shows that the Mtr-2 voltage sag's magnitude is more significant than Mtr-1.

The effectiveness of the control and the system performances under various sag compensations were demonstrated again. When the compensations for Mtr-2 were set at 10 %, 30 %, 50 %, 70 %, and 90 % of the motor inrush current, the Bus voltage improvement is depicted in this figure.

Another thing found in this study is that the compensation level applied to different MVIMs is unique. Voltage sag on Mtr-1 can be overcome by 70% compensation, but on Mtr-2, 70% compensation still causes a significant voltage drop. In Mtr-2, voltage sag can be overcome with 90% compensation

More detailed research results are shown in Table 2. The numbers shown in this table indicate the critical points of compensation on Mtr-1 and Mtr-2, including a comparison of the bus voltage conditions when the motor is started with compensation and without compensation. displayed. Another thing that was also displayed was the detailed number of the electrical current that flows from the Bus, flows from the inverter, and flows to the motor. The current flow shows that the compensation successfully mitigates the voltage sag at the system Bus. Supercapacitor voltage is also displayed in the table. When compensation is applied to the bus, Super-capacitor voltage reduces as the energy stored in the super-capacitor is channeled to the MVIM.

Table 2. Comparison of grid voltage sag for zero compensation, 10 %, 30 %, 50 % and 70 % compensation

Parameter	Un-Compensated		Compensated	
	Mtr-1	Mtr-2	Mtr-1	Mtr-2
Initial Lump Load 6.6 kV (Ampere)	124		124	
Compensation Percentage (%)	0%	0%	75%	90%
Bus current (Ampere)	1,090	1,241	322	315
Inverter Current (Ampere)	11	10	894	1,952
Motor Current (Ampere)	1,077	1,669	1,172	2,130
Percentage Current by Compensator	1.02	0.60	76.28	91.64
Voltage Sag (Volt)	5,809	4,939	6,318	6,287
Voltage Sag Duration (Second)	5.15	2.1	4.6	1.37
SC Initial Voltage (Volt)	850	876	850	798
SC End Voltage (Volt)	867	883	793	708

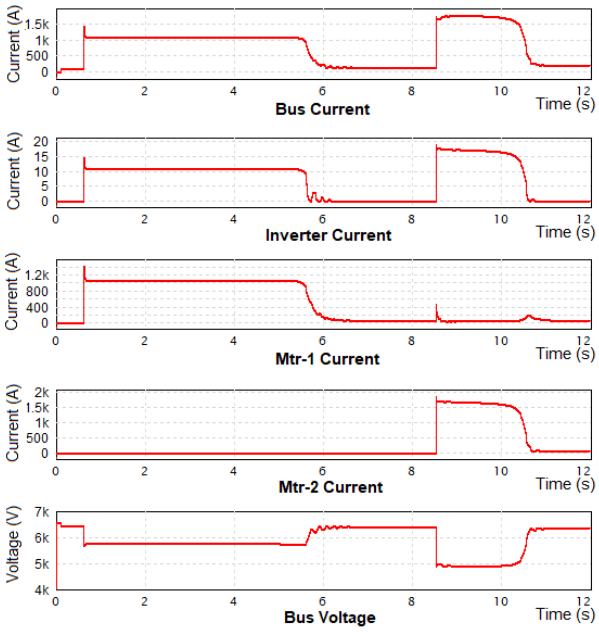

Figure. 14 Plant motors starting without compensation

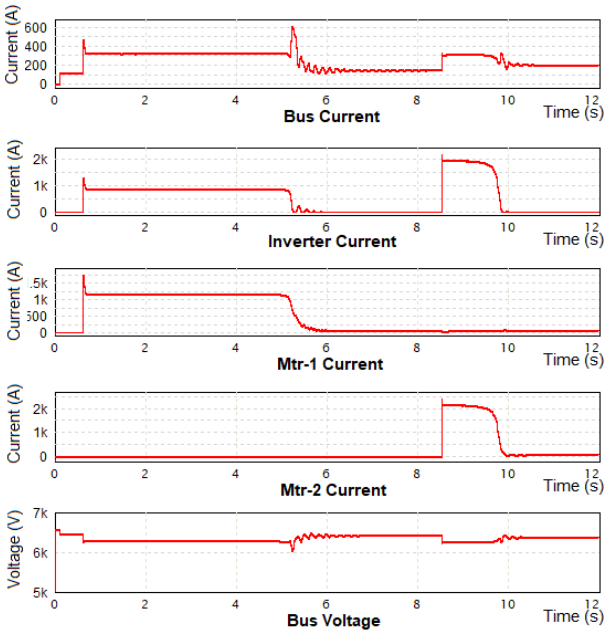

Figure. 15 Plant motors starting with compensation

The next test of the method proposed in this research is a test for starting a medium voltage induction motor (MVIM) sequentially. The test procedure is starting Mtr-1 and then following it with starting Mtr-2. The Mtr-2 will be started a few seconds after the Mtr-1 reaches its nominal speed.

This starting procedure is modeled from a common practice used in industry. This procedure is applied to test the reliability of the methods offered in this study. The results achieved are shown in Figs. 14 and 15. Fig. 14 is the result of the first sequential starting performed on Mtr-1 and Mtr-2 without compensation. Fig. 15 is the result of starting MVIM using compensation.

Bus Current in Fig. 14 is a graph of the current absorbed from the bus by the Lump load, Mtr-1, and Mtr-2, respectively. In the first 0.5 seconds, the electric current that flows is the load in low voltage equipment. This load serves to run the operations of a factory. This load includes a support system for running MVIM. A few seconds after, this Fig. shows the current on the Bus when Mtr-1 and Mtr-2 are started.

The inverter current in Fig. 14 is a graph of the current absorbed from the inverter by the same load as shown in the bus current. From the figures of bus current and inverter current, it can be seen that the Lump load is fully borne by the Bus. Bus current is shown that when Mtr-1 and Mtr-2 are started at seconds 0.5 and 8.5, the current in the Bus is very large, while at the same time, the Inverter current in the next figures small until it is close to zero.

Figures Mtr-1 current and Mtr-2 current of Fig. 14 are the graphs of the currents on Mtr-1 and Mtr-2 when both MVIMs are started. When these motors current are compared with the bus current and inverter current, it can be seen that the motor currents are almost entirely borne by the Bus. The last depicted figure in Fig. 14 shows the voltage on the Bus that supplies electrical energy for the Lump

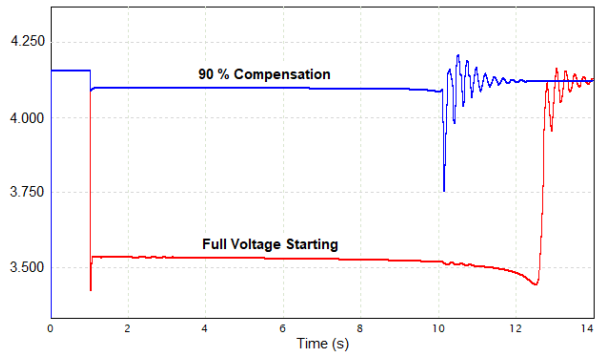

Figure. 16 Voltage sag on full voltage starting [5] and 90 % Compensation

load, Mtr-1, and Mtr-1 loads.

The first 0.5 seconds in this figure show the bus voltage, which is not much affected when receiving a lumped load. The voltage sag is seen in the next second due to the starting Mtr-1. This voltage sag occurs with a duration of about 5 seconds. At 8.5 seconds, a deeper voltage sag appears, but with a shorter duration than the first voltage sag. These two voltage sags are caused by the inrush current that occurs when starting Mtr-1 and Mtr-2.
Since the magnitude of the voltage sag is bigger than 5% of the nominal voltage, the voltage sag causes power quality problems on the Bus.

Fig. 15 is the final result achieved in this study. This image provides the same picture as Fig. 14, except that the data provided is the result of the inverter with compensation.

Mtr-1 current in Fig. 15 shows the magnitude of the current Mtr-1, which is the sum of the currents on the Bus current and Inverter current in this figure. A similar figure is shown in Mtr-2 current. The Mtr-2 current in the figure is the sum of the Bus current and the inverter current in Fig. 15. The amount of inverter current is in accordance with the percentage of compensation given. This shows that the electric current injected by the inverter successfully bears part of the inrush current load. The effect is reducing the voltage sag that occurs in Bus. In the bus voltage figure, it can be seen that the bus voltage variation does not change much. Thus the voltage sag on the Bus can be mitigated using the compensator proposed in this research.

4.2 System validation and comparison

The proposed method in this paper is validated and compared to the researches in the reference section. Among the various mitigation methods to overcome the inrush current of induction motors as carried out in research [5, 6, 8, 11]. The method used in research [5] is the most up-to-date and completed with detailed motor and system specifications used in the plant. Paper research [5] uses a 4157 hp 4160 Volt induction motor supplied from a 7.5 MVA 6.4%Z transformer. By using the Full Voltage Starting method, obtained a voltage drop of 15% with a duration of 12 seconds. Simulations were made with the data of grid voltage, voltage drop, and supply voltage recovery time using the full voltage method in paper [5]. The results of this simulation are used as initial conditions to be compared with the Inrush current improvement using the compensation method proposed in this study. The results of this initial condition simulation are shown as a Full Voltage Starting graph in Fig. 16.

From several induction motor starting methods discussed in research [5], the best result achieved is the fully rated ASD method. By using this method, the result is a voltage drop of 2% with a duration of 8 seconds. The fully rated ASD method is used as a comparison to prove that the inrush current compensation method proposed in this study produces a smaller voltage drop.

The energy required to compensate for the voltage drop is calculated using equations (1), (2), and (3). Using the same method as used in chapter 2.2 of this paper, the energy required to improve the voltage drop from 15% to 2% and reduce the duration of the voltage drop from 12 seconds to 8 seconds can be calculated. The energy obtained from this calculation is 1.16 kWH. This amount of energy is smaller than the amount of energy stored in the supercapacitor proposed in this study, which is 5.54 kWH. By entering a compensation value of 90 %, the voltage drop on the grid is 4095 Volts (1.56 %) with a duration of 8.59 seconds.

The voltage drops of 1.5% resulting from this inrush current compensation are smaller than the 2% voltage drop obtained by the fully rated ASD method in the paper [5]. On the other hand, the duration of the voltage drop resulting from the fully rated ASD method is 8 seconds, 0.59 seconds shorter than the duration of the voltage
drop using the inrush current compensation method. According to standards [3, 4], the recommended voltage drop limit is 5%, hence the result satisfies the requirement. The detailed results of this comparison are shown in Table 3.

The main concern of the inrush current compensation method proposed in this study is the additional function of the existing PV Farm. By coordinating the current and voltage at the time the motor is started, some portion of the inrush current that occurs can be supplied by the system in the proposed method. The effect that occurs is that the

Table 3. Voltage sag parameters of full voltage, ASD [5] and compensator methods

Parameter	Full Voltage	ASD [5]	Compensator
Voltage Sag Magnitude (Volt)	3.536	4.076	4.095
Voltage Sag Percentage (%)	15	2	1.58
Voltage Sag Duration (Second)	12	8	8.59
Percentage Compensation	-	-	90
SC Initial Voltage (Volt)	-	-	850
SC End Voltage (Volt)	-	-	830

voltage sag on the network can be mitigated. This process is different from the motor starter. The initial design of the motor starter to help start the induction motor. The comparison presented in this sub-section is to verify the results of the research conducted.

5. Conclusions

The effect of the ancillary function of Plant PV Farm to overcome the Voltage Sag phenomenon due to the inrush current of the induction motor has been investigated and presented in this paper. By utilizing the energy stored in the supercapacitor and controlling the current through the voltage source inverter, the inrush current in the grid can be reduced so that the voltage sag that occurs is reduced in both magnitude and duration. It was clearly monitored that on the 6.600 Volt grid voltage, during the starting of MVIM – Mtr-1, the grid voltage drops to 5.941 volts, and by using the proposed method, it can be improved to 6.384 volts. This 6.384 volt is less than 5 %. Improvement also can be seen in the duration of the voltage sag reduce from 5.3 seconds become 4.9 seconds. A similar result is achieved for the Mtr-2. Voltage sag can be maintained for not less than 6.270 Volt.

In this study, the production process in the factory is also simulated by starting the MVIM motors sequentially. The second motor is being started a few seconds after the first motor has reached its nominal speed. The result achieved is system voltage quality can be maintained to follow the standard requirements.

Inverter specifications used in the industry generally include impulse capacity or surge capacity. Impulse capacity or surge capacity is the ability of the inverter to deliver large amounts of power in a short time. This impulse capacity / Surge capacity in the inverter can be used as an object of further research to increase its capacity so that it can be used as a compensator.

Further research could be carried out widely by improving the controller, so that the system's functionality can be expanded and can overcome other power quality problems, including swell problems and harmonic problems that often arise due to the massive use of the FACTS devices.

Appendix

Table 4. List of notations used in this paper

52	ANSI standard devices number for AC Circuit Breaker
C	Compensation
CT	Current Transformer
FACTS	Flexible AC Transmission System
IM	Induction Motor
INV	Inverter
LV	Low Voltage
MFR	Multi-Function Relay
Mtr-	Induction Motor -
MV	Medium Voltage
MVIM	Medium Voltage Induction Motor
PT	Potential Transformer
PV	Photo Voltaic
SC	Supercapacitor
VS	Voltage Sag
XFMR	Transformer

Conflicts of interest

The authors declare no conflict of interest.

Author contributions

Conceptualization, Indra Budi Hermawan, Mochamad Ashari, Dedet Candra Riawan; methodology, Indra Budi Hermawan, Mochamad Ashari, Dedet Candra Riawan; validation, Indra Budi Hermawan, Dedet Candra Riawan; formal analysis, Indra Budi Hermawan, Mochamad Ashari, Dedet Candra Riawan; investigation, Indra Budi Hermawan; resources, Indra Budi Hermawan; writing original draft preparation, Indra Budi Hermawan; writing review and editing, Indra Budi Hermawan, Mochamad Ashari, Dedet Candra

Riawan; visualization, Indra Budi Hermawan. All authors have read and agreed to the published version of the manuscript.

Acknowledgments

This research was funded by the Ministry of Research, Technology, and Higher Education Indonesia, under the scheme of PDD (Penelitian Disertasi Doktor).

References

[1] I. Boldea and S. A. Nasar, *The Induction Machine Handbook*, CRC Press, 2002.

[2] M. J. Melfi and S. D. Umans, "Squirrel-Cage Induction Motors_Understanding Starting Transients", *IEEE Industry Applications Magazine*, pp. 28-36, Nov/Dec 2012.

[3] Menteri ESDM RI, "Aturan Jaringan Sistem Tenaga Listrik (Grid Code)", *Peraturan Menteri Energi dan Sumber Daya Mineral Republik Indonesia*, No. 20, p 30, 2020.

[4] IEEE, "IEEE Guide for Voltage Sag Indices", *IEEE Std 1564 -2014, Transmission and Distribution Committee*, p. 10.

[5] A. H. VanderMeulen, T. J. Natali, T. J. Dionise, G. Paradiso, and K. Ameele, "Exploring New and Conventional Starting Methods of Large Medium-Voltage Induction Motors on Limited kVA Sources", *IEEE Transactions On Industry Applications*, Vol. 55, No. 5, pp. 4474-4482, September/October 2019.

[6] K. LeDeux, P. W. Visser, J. D. Hulin, H. Nguyen, "Starting Large Synchronous Motor in Weak Power System", *IEEE Transaction on Industry Applications*, Vol. 51, No. 3, pp. 2676-2682, May/June 2015.

[7] Y. H. Song and A. T. Johns, "Flexible AC Transmission System (FACTS)", *The Institue of Electrical Engineers, London*, 1999.

[8] D. S. Padimiti, M. B. Cristian Sr, and J. Jarvinen, "Effective Transient-Free Capacitor Switching (TFCS) for Large Motor Starting on MV Systems", *IEEE Transaction on Industry Applications*, Vol. 55, No. 1, pp. 1012-1020, January 2019.

[9] M. Khederzadeh, "Mitigation of the impact of transformer inrush current on voltage sag by TCSC", *Elsevier, Electric Power System Research*, Vol. 80, pp. 1049-1055, 2010.

[10] B. Singh, P. Jayaprakash, D. P. Kothari, A. Chandra, and K. A. Haddad, "Comprehensive Study of DSTATCOM Configurations", *IEEE Transaction on Industrial Informatics*, Vol. 10, No. 2, pp. 854-870, 2014.

[11] J. R. Ramamurthy, S. Kolluri, D. J. Mader, and E. Camm, "Mitigation of Motor Starting Voltage Sag using Distribution-Class STATCOM", In: *Proc. of IEEE/PES Transmission and Distribution Conference and Exposition (T&D)*, 2018.

[12] L. Li and X. Zhang, "Study on STATCOM Principle and Control Strategy under Short Circuit Fault", In: *Proc. of IEEE, International Conference on Mechatronics and Automation, Japan*, pp. 1187-1191, 2017.

[13] N. H. Rajak and V. J. Rupapara, "Voltage Sag Mitigation on Power Distribution System Using D-Statcom", *ITSI Transaction on Electrical and Electronics Engineering (ITSI-TEEE), ISSN(PRINT)*, pp. 2320-8945, Vol. 1, Issue 3, 2013.

[14] C. Han, A. Q. Huang, M. E. Baran, S. Bhattacharya, W. Litzenberger, L. Anderson, A. L. Johnson and A. A. Edris, "STATCOM Impact Study on the Integration of a Large Wind Farm into a Weak Lop Power System", *IEEE Transaction on Energy Conversion*, Vol. 23 No. 1, pp. 226-233, 2008.

[15] P. Li, L. Xie, J. Han, S. Pang, and P. Li, "A New Compensation Philosophy for Dynamin Voltage Restorer to Mitigate Voltage Sags using Three-Phase Voltage Ellipse Parameters", *IEEE Transactions on Power Electronics*, Vol. 33, No. 2, pp. 1154-1166, February 2018, doi 10.1109/TPEL.2017.2676681.

[16] A. Kiswantono, E. Prasetyo, and Amirullah, "Comparative Performance of Mitigation Voltage Sag/Swell and Harmonics Using DVR-BES-PV System with MPPT-Fuzzy Mamdani/MPPT-Fuzzy Sugeno", *International Journal of Intelligent Engineering and Systems*, Vol. 12, No. 2, 2019, doi: 10.22266/ijies2019.0430.22

[17] S. Galeshi and H. I. Eini, "Dynamic Voltage Restorer Employing Multilevel Cascaded H-Bridge Inverter", *The Institution of Engineering and Technology* (*IET) Journal on Power Electronics*, pp. 1-9, 2016.

[18] D. I. Brandao, F. E. G. Mendes, R. Ferreira, S. M. Silva, and I. A. Pires, "Active and Reactive Power Injection for Three-Phase – Four-Wire Inverter During Symmetrical/Asymmetrical Voltage Sags", *IEEE Transactions on Industry Applications*, Vol. 55. No. 3, pp. 2347-2355, May/Jun 2019.

[19] L. Wang, C. S. Lam, and M. C. Wong, "Multifunctional Hybrid Structure of SVC and Capacitive Grid-Connected Inverter (SVC//CGCI) for Active Power Injection and Nonactive Power Compensation", *IEEE Transactions On Industrial Electronics*, Vol. 66, No. 3, pp. 1660-1670, March 2019.

[20] A. Rizqiawan, P. Hadi, and G. Fujita, "Development of Grid-Connected Inverter Experiment Modules for Microgrid Learning", Energies, Vol. 12, No. 476, 2019, doi:10.3390; en12030476.

[21] Y. Ru, J. Kleissl, and S. Martinez, "Storage Size Determination for Grid-Connected Photovoltaic Systems", *IEEE Transactions on Sustainable Energy*, Vol. 4, No. 1, pp. 68-81, 2013.

[22] J. Tant, F. Geth, D. Six, P. Tant, and J. Driesen, "Multiobjective Battery Storage to Improve PV Integration in Residential Distribution Grids", *IEEE Transactions on Sustainable Energy*, Vol. 4, No. 1, pp. 182-191, 2013.

[23] P. Thounthong, A. Luksanasakul, P. Koseeyaporn, and B. Davat, "Intelligent Model-Based Control of a Standalone Photovoltaic/Fuel Cell Power Plant WithSupercapacitor Energy Storage", *IEEE Transactions on Sustainable Energy*, Vol. 4, Issue 1, pp. 240-249, Jan. 2013.

[24] D. Somayajula and M. L. Crow, "An Ultracapacitor Integrated Power Conditioner for Intermittency Smoothing and Improving Power Quality of Distribution Grid", *IEEE Transactions on Sustainable Energy*, Vol. 5, No. 4, pp. 1145-1155, 2014.

[25] I. H. Panhwar, K. Ahmed, M. Seyedmahmoudian, A. Stojcevski, B. Horan, S. Mekhilef, A. Aslam, and M. Asghar, "Mitigating Power Fluctuations for Energy Storage in Wind Energy Conversion System Using Supercapacitors", *IEEE Access, Special Section on Evolving Technologies in Energy Storage Systems for Energy Systems Applications*, pp. 189747-189760, 2020.

[26] L. Wang, F. Bai, R. Yan, and T. K. Saha, "Real-Time Coordinated Voltage Control of PV Inverters and Energy Storage for Weak Networks with High PV Penetration", *IEEE Transactions on Power Systems*, Vol. 33, No. 3, pp. 3383-3395, 2018.

[27] Y. Yang, Q. Ye, L. J. Tung, M. Greenleaf, and H. Li, "Integrated Size and Energy Management Design of Battery Storage to Enhance Grid Integration of Large-Scale PV Power Plants", *IEEE Transactions on Industrial Electronics*, Vol. 65, No. 1, pp. 394-402, 2018.

[28] S. Teleke, M. E. Baran, S. Bhattacharya, and A. Q. Huang, "Rule-Based Control of Battery Energy Storage for Dispatching Intermittent Renewable Sources", *IEEE Transactions on Sustainable Energy*, Vol.1 No. 3, pp. 117-124, 2010.

[29] L. Wang, Q. S. Vo, and A. V. Prokhorov, "Stability Improvement of a Multimachine Power System Connected with a Large-Scale Hybrid Wind-Photovoltaic Farm Using a Supercapacitor", *IEEE Transactions on Industry Applications*, PSEC-0076, pp. 1-9, 2017, doi 10.1109/TIA.2017.2751004.

[30] O. M. Akeyo, V. Rallabandi, N. Jewell, D. M. Ionel, "The Design and Analysis of Large Solar PV Farm Configurations with DC Connected Battery Systems", *IEEE Transactions on Industry Applications*, Vol. 56, No.3, pp. 2903-2912, May/June 2020, doi 10.1109/TIA.2020. 2969102.

[31] S. Marhraoui, A. Abbou, Z. Cabrane, S. E. Rhaili, N. Hichami, "Fuzzy Logic-Integral Backstepping Control for PV Grid-Connected System with Energy Storage Management", *International Journal of Intelligent Engineering and Systems*, Vol. 13, No. 3, 2020, doi: 10.22266/ijies2020.0630.33.

[32] M.H. Rashid, *Power Electronics Handbook*, Third Edition, Copyright 2011, Elsevier Inc, 2011.